

Cuff-less Calibration-free Blood Pressure Estimation under Ambulatory Environment using Pulse Wave Velocity and Photoplethysmogram Signals

Haruyuki Sanuki¹, Rui Fukui¹, Tsukasa Inajima² and Shin'ichi Warisawa¹

¹Graduate School of Frontier Sciences, The University of Tokyo, 5-1-5 Kashiwanoha, Kashiwa-shi, Chiba 277-8563, Japan

²The University of Tokyo Hospital, 7-3-1 Hongo, Bunkyo-ku, Tokyo 113-8655, Japan

Keywords: Blood Pressure Monitoring, Pulse Wave Velocity, Photoplethysmogram, Electrocardiogram.

Abstract: This paper presents a blood pressure estimation method based on pulse wave velocity (PWV). Although there are a variety of methods based on PWV to estimate blood pressure, most of them require calibration per patient, and the patient has to remain still. The goal of our research is to develop a calibration-free blood pressure estimation method that is applicable not only during rest but also during exercise. To accomplish our goal, we extracted properties of blood vessels from photoplethysmogram (PPG) signals, and compared several regression models, such as the deductive model based on blood vessel physics equation, and the inductive model based on machine learning. Twenty-four participants performed exercise, measuring blood pressure, electrocardiogram (ECG) and PPG. The best result showed that the mean error for the estimated systolic blood pressure (SBP) against cuff-based blood pressure was 0.18 ± 8.68 mmHg. Although there was not a big difference between the regression models, PWV and Augmentation Index are effective features to estimate SBP. In addition to this, Heart Rate was effective only for the young men, and height ratio of c-wave to a-wave of acceleration pulse wave might be effective for elderly men. These results suggest that our proposed method has the potential for cuff-less calibration-free blood pressure estimation which include measurements during rest and exercise.

1 INTRODUCTION

In recent years, the number of hypertension patients has increased, and around 40% of adults aged 25 and over were estimated to have hypertension (World Health Organization, 2014). Hypertension can lead to various diseases such as a life-threatening heart disease, cardiovascular diseases (CVDs), and renal insufficiency. Since most people are not aware of their hypertension, they are not treated in time. Monitoring one's blood pressure is required for the prevention, early detection, and early recovery of hypertension.

However, single blood pressure measurement is the mainstream in hospitals or at home. It is difficult to monitor the changes of blood pressure, especially indicators like short-term changes and changes during the day, which are important to diagnose a patient's body. Moreover, white-coat hypertension, which leads to high blood pressure when measured in the medical environment, could cause misdiagnosis. To diagnose and treat such patients

properly, continuous blood pressure monitoring is required.

Nowadays, Ambulatory Blood Pressure Monitoring (ABPM) is used for continuous blood pressure measurement. Figure 1 shows ABPM equipment. ABPM measures blood pressure by a cuff every 15 minutes or so. It is rather uncomfortable and the patient has to remain still.



Figure 1: ABPM equipment.

The method based on pulse wave velocity (PWV) has been intensively studied because of its potential

for tracking blood pressure change continuously without a cuff (Mukkamala et al., 2015). PWV is the velocity of an arterial pulse propagating through the arterial wall and can easily be calculated from Pulse Transit Time (PTT). PTT is the time interval between an R-wave peak of electrocardiogram (ECG) and a particular point of photoplethysmogram (PPG). PWV is obtained by dividing distance from the heart to a particular peripheral site by PTT.

Based on previous researches, a formula which takes continuity equation and Navier-Stokes equation estimates systolic blood pressure (SBP). The formula is as follows (Lopez, 2010, Inajima, 2012).

$$SBP = b_1 v_{pwv}^2 + b_2 \quad (1)$$

v_{pwv} is the pulse wave velocity, and coefficients b_1 and b_2 are parameters related to individual blood vessel properties. Traditionally, the coefficients are calibrated by measuring blood pressure and PWV beforehand.

Gesche et al. established a model with PWV to estimate systolic blood pressure (SBP) during exercise with initial calibration, and the standard deviation of estimation error (SD) was 10.1 mmHg (Gesche, 2012). Ding et al. established a model with PWV and photoplethysmogram intensity ratio to estimate blood pressure during rest with initial calibration, and SD was 5.21 mmHg for SBP and 4.06 mmHg for diastolic blood pressure (DBP) (Ding, 2015). Kauchuee et al. investigated the relationship between PTT and blood pressure and found that non-linear models are better than linear models. Kachuee's model without calibration during rest achieved 16.17 mmHg for SBP and 8.45 mmHg for DBP (Kachuee, 2015).

Although there are a variety of methods based on PWV to estimate blood pressure, the application of the PWV-based method has several problems. First, individual blood vessel properties differ from person to person. Most of the methods, therefore, require calibration per person. Secondly, current methods still lack application during exercise. Thirdly, there is not enough accuracy of blood pressure measurement based on PWV for medical use.

The objective of our study is to establish a calibration-free blood pressure estimation method based on PWV during rest and exercise. To achieve the objective, we extracted properties of blood vessels from photoplethysmogram (PPG) signals and compared several regression models, such as the deductive model based on blood vessel physics

equation and the inductive model based on machine learning.

In this research, we focused on SBP that is superior to Diastolic blood pressure as a predictor of CVDs (Mourad, 2008).

This paper is organized as follows. Chapter 2 shows an overview of our methodology including peak detection method, feature extraction, regression models and evaluation method. Chapter 3 explains the experiment, and Chapter 4 describes the result. Lastly, Chapter 5 is the conclusion of this research and future perspectives.

2 METHOD

Our method estimates SBP by using ECG and PPG. The method is demonstrated in Figure 2. While extracting features from ECG and PPG signals, we use peak detection to extract features automatically. Therefore, we first explain the peak detection method before feature extraction.

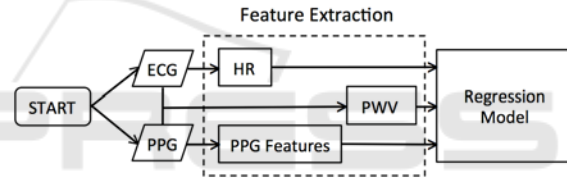


Figure 2: Overview of the method to estimate SBP.

2.1 Peak Detection

In order to extract features from ECG and PPG signals automatically, we need to build a robust pattern-matching model. Therefore, we applied Continuous Wavelet Transform (CWT), which is widely used for R spike detection (Legarreta, 2005) and PPG waveform analysis (Fan, 2011). The Mexican Hat wavelet was selected as the mother wavelet, because of its similarity with the ECG and PPG signals (Daubechies, 1992). We found optimal scales for each signal using annotations provided on small data. Figure 3 shows an R spike detection of ECG signal, and Figure 4 shows a foot point detection of PPG signal.

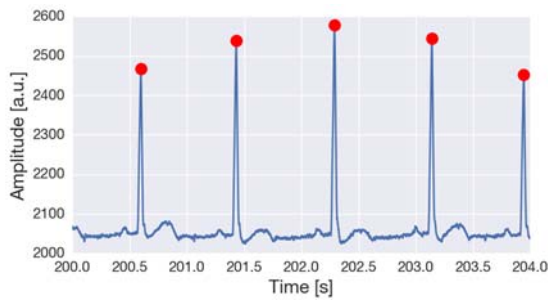


Figure 3: R spike detection of ECG signal.

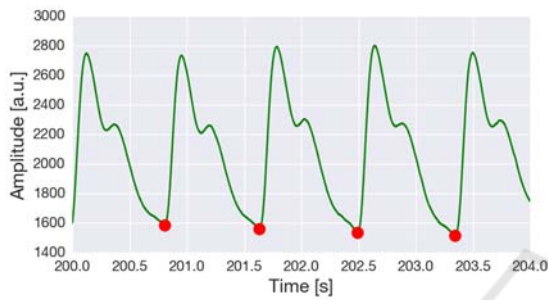


Figure 4: Foot point detection of PPG signal.

2.2 Feature Extraction

We extract Heart Rate (HR) from ECG signal, PPG features from PPG signal, and PWV from ECG and PPG signals.

2.2.1 PWV and HR

PWV was calculated by dividing the participant's height by time interval between R-wave peak of ECG and three points of PPG, which are the steepest slope of the corresponding upstroke (PWV_m), the maximum point (PWV_p), and the minimum point (PWV_b), as shown in Figure 5. HR is calculated by the time interval between the nearest R spikes.

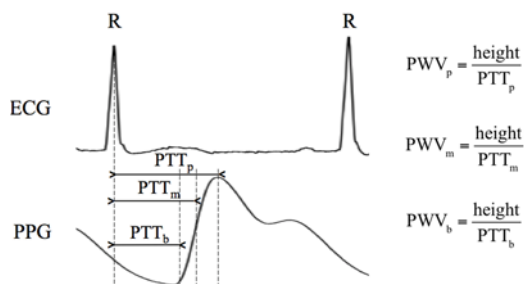


Figure 5: Definition of each PWV.

2.2.2 PPG Features

The PPG signal reflects the blood volume of the

vessel, measured by red, green or infrared light, which is irradiated into the tissue and is absorbed or reflected. The features extracted from PPG signal have relationships with blood vessel conditions (Elgendi, 2012). Most researches extract features from velocity pulse waves (first derivative) and acceleration pulse waves (second derivative) of the PPG signal to interpret the original PPG signal (Takazawa, 1998). In this research, features are extracted from volume pulse waves and acceleration pulse waves.

In volume pulse waves, Inflection Point Area Ratio (IPA), Augmentation Index (AI), Crest Time (CT), and Large Artery Stiffness Index (LASI) are extracted.

- Inflection Point Area Ratio (IPA): IPA is the ratio of the four pulse areas between the selected points, S1, S2, S3 and S4, which are shown in Figure 6. IPA is used as an indicator of the total peripheral resistance (Wang, 2009). In this research, it is proposed to use the ratio of S2, S3, and S4 to S1.

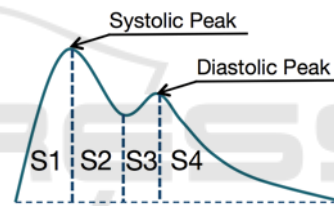


Figure 6: Definition of S1, S2, S3 and S4.

- Augmentation Index (AI): AI is the ratio of the height of the diastolic peak to height of the systolic peak (Figure 7). AI is a measure of the wave reflection and arterial stiffness (Takazawa, 1998).
- Crest Time (CT): CT is the time interval between the foot point and the systolic peak (Figure 7). CT is an important feature for classifying cardiovascular diseases (Alty, 2007).
- Large Artery Stiffness Index (LASI): LASI is the time interval between the systolic peak and the diastolic peak (Figure 7). LASI is related to large artery stiffness (Elgendi, 2012).

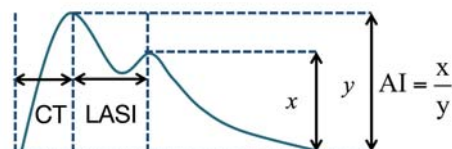


Figure 7: Definition of AI, CT, and LASI.

As Figure 8 shows, an acceleration pulse wave includes five component waves, namely a-wave, b-wave, c-wave, d-wave and e-wave. The type of acceleration pulse waveform varies depending on the blood vessel conditions. The height ratios and the time intervals of each wave are extracted.

- Height ratio b/a, c/a, d/a, e/a; each height ratio reflects arterial stiffness. If arterial stiffness increased, b/a would increase and c/a, d/a, e/a would decrease (Takazawa, 1998).
- Time interval between a-wave and b-wave (a_b), a-wave and c-wave (a_c), a-wave and d-wave (a_d), a-wave and e-wave (a_e). Time interval of each wave describes acceleration pulse waveform.

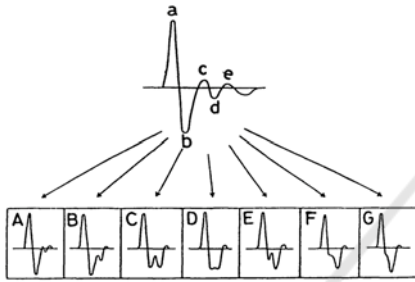


Figure 8: Acceleration pulse wave waveform. Waveform differs depending on the vascular status (Homma, 1992).

In this research, features are selected in each regression model by greedy forward selection (Caruana, 1994).

2.3 Regression Model

In this research, two main approaches are taken to choose a better regression model. One is the deductive model based on blood vessel physics equation, which is represented as Eq. (1), while the other is the inductive model based on machine learning.

2.3.1 Model based on Physics Equation

As shown in Eq. (2), the extracted features determine individual blood vessel condition parameters b_1 and b_2 . We use PWV_m as pulse wave velocity in Eq. (2).

$$SBP = (a_{10} + a_{11}x_1 + a_{12}x_2 + \dots)v_{pwv}^2 + (a_{20} + a_{21}x_1 + a_{22}x_2 + \dots) \quad (2)$$

a_{ij} is the partial regression coefficient and x_{ij} is the extracted feature. We named this model as LR.

2.3.2 Model based on Machine Learning

We use the inductive model based on machine learning, not using a hypothesis but learning only from the data.

Three regression models are selected, K-Nearest Neighbours (KNN), Random Forest (RF) and Linear Support Vector Machine (SVM).

- K-Nearest Neighbours (KNN): KNN is the simplest nonparametric decision procedure, and predicts a sample data by using its K-nearest neighbors (Cover, 1967).
- Random Forest (RF): RF is a combination of tree predictors, such that each tree depends on the values of random features sampled independently and with the same distribution for all trees in the forest (Breiman, 2001).
- Linear Support Vector Machine (SVM): SVM is the algorithm that maximizes the margin between the training patterns and the decision boundary, and is widely used for classification and regression problems (B. E. Boser, 1992).

Each hyper-parameter is optimized by cross validation.

2.4 Evaluation

As shown in Figure 9, in order to evaluate the accuracy without any individual dependency, each participant's data is taken out as test data in turn, and is evaluated with the data of remaining train data.

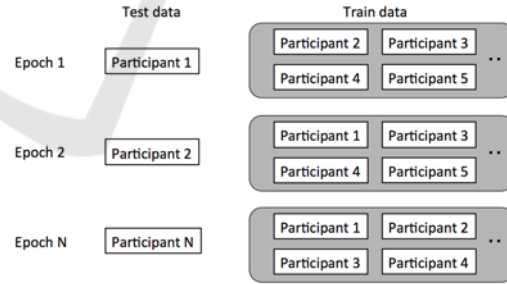


Figure 9: Cross-validation for independent validation.

Though it is better to split data into three sets, which are training data, validation data and test data, we will split data into two sets, train data and test data, because of the small sample size.

3 EXPERIMENTS

We conducted experiments on 18 young men (22.9±1.2 years) and six elderly men (43.3±9.3

years). All participants underwent an exercise test for 28 minutes on a bicycle ergometer, and four minutes of rest before and after the test, acquiring ECG, PPG and SBP by sphygmomanometer. The timing of load increase and decrease is shown in Figure 10. The load was adjusted corresponding to their exercise capacity.

Participants wear the ECG sensor surrounding the heart, PPG sensor at the right index finger, and a sphygmomanometer with a cuff (Tango M2 from SunTech Medical) on the left arm. SBP was measured every two minutes by a cuff and the sampling rate of ECG and PPG measurements were both at 1 kHz. ECG and PPG signals are sampled at the same time with same microcomputer that would guarantee the synchronization. As a reference, participants wear PPG sensor at the right earlobe and finger cuff (ClearSight from Edwards Lifesciences) on the right middle finger. Figure 11 shows a schematic of the experimental set-up. All the participants gave their informed consent prior to the experiment.

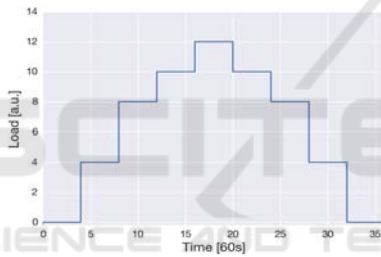


Figure 10: Exercise weight transition.

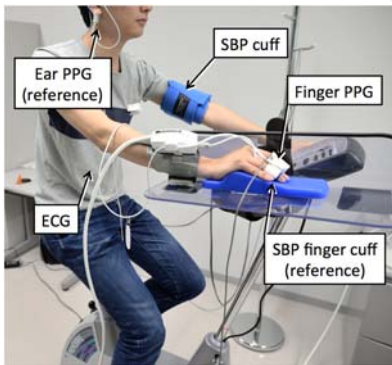


Figure 11: Schematic of the experimental set-up.

4 RESULTS

The SBP distribution histogram is shown in Figure 12, including 341 SBP measurements. The mean SBP measured by the sphygmomanometer was

128.05±16.90 mmHg.

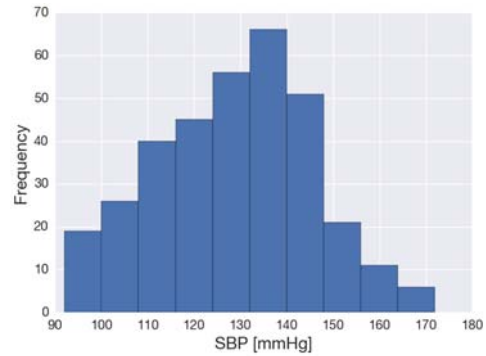


Figure 12: Histogram of SBP measurements.

We defined two groups, Group A only contains young men and Group B contains both, young and elderly men. The reason for not grouping elderly men is that the sample size was not large enough.

The results from various regression models are shown in Table 1. Although KNN showed the best regression model for estimating SBP, there was not a big difference between the deductive model based on blood vessel physics equation and the inductive model based on machine learning.

Table 1: Standard Deviation of estimation error for each regression model.

	LR	KNN	SVM	RF
Group A [mmHg]	8.68	8.65	8.74	9.28
Group B [mmHg]	8.79	8.68	8.75	9.20

Table 2 shows the feature subset that is selected by each regression model and Eq. (3) shows the deductive model based on the blood vessel physics equation. While PWV is an important feature in each group, as expected, AI also appeared to be an important feature. HR is only effective for young men, and the height ratio of c-wave to a-wave of acceleration pulse wave might be effective for elderly men.

Group A

$$SBP = (13.0HR + 1.8S3/S1)v_{pwv}^2 - 3.3AI + 125.9 \quad (3)$$

Group B

$$SBP = (-0.3c/a + 11.2)v_{pwv}^2 - 4.8AI + 128.0$$

Hereinafter, KNN is selected as the most accurate in the regression model evaluation, according to Table 2. Figure 13 shows the plot of cuff-based SBP and estimated SBP of Group B, and the correlation coefficient was $r=0.86$ (p -value<0.01). Figure 14 gives the Bland-Altman plot, comparing for the

Table 2: The feature subset that is selected by greedy forward selection in each regression model. Group A is the young men group and Group B is the young and elderly men group. \circ is the selected feature.

		PWV _b	PWV _m	PWV _p	HR	IPA (S2/S1, S3/S1, S4/S1)	AI	CT	LASI	Height ratio (b/a, c/a, d/a, e/a)	Time interval (a, b, a, c, a, d, a, e)
A	LR	-	-	-	$HR \times PWV_m^2$	$S3/S1 \times PWV_m^2$	\circ	-	-	-	-
	KNN	\circ	\circ	-	\circ	-	\circ	-	-	-	a_b
	SVM	-	\circ	-	\circ	-	\circ	-	\circ	-	a_c, a_e
	RF	-	\circ	-	\circ	-	\circ	-	-	-	-
B	LR	-	\circ	-	-	-	\circ	-	-	$c/a \times PWV_m^2$	-
	KNN	\circ	\circ	-	-	-	\circ	-	-	e/a	-
	SVM	\circ	\circ	-	-	-	\circ	-	-	c/a	a_e
	RF	-	\circ	-	-	-	\circ	-	-	c/a	-

performance of the proposed method with the cuff-based measurements of Group B. A total of 94.73% of the measurements lies in the limits of agreement ($1.96 \times SD$).

5 DISCUSSIONS

Previous researches show an effective model with initial calibration during rest or exercise. The present study proposed the calibration-free blood pressure estimation method based on PWV during rest and exercise and the method achieved grade C as IEEE standard requirement. Moreover, we showed that PPG features, especially AI, are effective to estimate SBP. Although we tried to find the cause of large error lying out of the limits of the agreement in particular subjects, we were not able to find it out because of the small sample size.

Some limitations remain in this research. One is that our proposed model are validated by cuff-based blood pressure but should be validated by invasive arterial blood pressure. Furthermore, the proposed model applied to 18 young men (22.9 ± 1.2 years) and 6 elderly men (43.3 ± 9.3 years), which is not enough to pass the standard requirement. Finally, the situation is limited to rest and specific exercise compared to ambulatory environment.

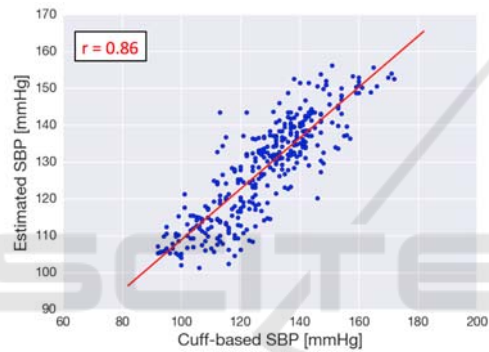


Figure 13: Correlation plot of SBP.

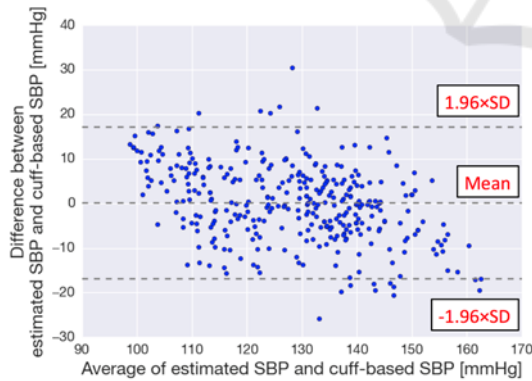


Figure 14: Bland-Altman plot of SBP.

Our proposed model for Group B, which contains young and elderly men, showed that the mean error was 0.18 ± 8.68 mmHg, and the mean absolute difference (MAD) was 6.93 mmHg, achieving grade C as IEEE standard requirement (IEEE Standards Association, 2014).

6 CONCLUSIONS

In this research, we presented a calibration-free blood pressure estimation method under ambulatory environment. Using PPG features, especially AI, enhances the accuracy of blood pressure estimation. HR is only effective to estimate SBP for young men, and height ratio of c-wave to a-wave of acceleration pulse wave might be effective in elderly men. According to the IEEE standard, the proposed method achieved grade C in the SBP estimation.

In order to apply our method to daily use, we have to address some issues.

- Validation should be conducted with a larger sample size, including female participants, elderly participants and hypertensive patients,

to pass the standard requirement and to investigate the difference between the hypertensive participants and non-hypertensive participants as well as the elderly participants and the young participants.

- Although we considered the situation of rest and exercise, other situations that could cause blood pressure changes, such as stressful situations, should be taken into account.
- Motion artifact can obscure the waveform of PPG signals obtained from the hand for daily use. Therefore, obtaining PPG signal from different specific portions of a body that are less affected by motion artifact should be considered.

ACKNOWLEDGMENT

This research was supported by Pacific Medico Co. for providing ECG and PPG measurement devices.

REFERENCES

- Alty, S., Angarita, J. N., Millasseau, S., Chowienczyk P., 2007. Predicting arterial stiffness from the digital volume pulse waveform. *IEEE Transactions on Biomedical Engineering*, 54(12), pp.2268–2275.
- Boser, B. E., Guyon, I. M., Vapnik, V.N., 1992. A training algorithm for optimal margin classifiers. *Proceedings of the fifth annual workshop on Computational learning theory - COLT '92*, pp.144-152.
- Breiman, L., 2001. Random forests. *Machine Learning*, 45(1), pp. 5-32.
- Caruana, R. Freitag, D., 1994. Greedy attribute selection. *Machine Learning Proceedings 1994*, pp.28–36.
- Cover, T. M., Hart, P. E., 1967. Nearest neighbor pattern classification. *IEEE Transactions on Information Theory*, 13(1), pp.21-27.
- Daubechies, I., 1992. Ten lectures on wavelets. *Society for Industrial and Applied Mathematics Philadelphia, PA*.
- Ding, X. R., Zhang, Y. T., Liu, J., Dai, W. X., Tsang, H. K., 2016. Continuous cuffless blood pressure estimation using pulse transit time and photoplethysmogram intensity ratio. *IEEE Transactions on Biomedical Engineering*, 63(5), pp.964–972.
- Elgendi, M., 2012. On the analysis of fingertip photoplethysmogram Signals. *Current Cardiology Reviews*, 8(1), pp.14–25.
- Fan, Z., Zhang, G., Liao, S., 2011. Pulse wave analysis. *Advanced Biomedical Engineering*, pp.21-40.
- Gesche, H., Grosskurth, D., Kuchler, G., Patzak, A., 2012. Continuous blood pressure measurement by using the pulse transit time: comparison to a cuff-based method. *European Journal of Applied Physiology*, 112(1), pp.309–315.
- Homma, S., Ito, S., Koto, T., Ikegami, H., 1992. Relationship between accelerated plethysmogram, blood pressure and arteriolar elasticity. *Japanese Journal of Physical Fitness and Sports Medicine*, 41(1), pp.98–107.
- Inajima, T., Imai, Y., Shuzo, M., Lopez, G., Yanagimoto, S., Iijima, Katsuya, Morita, H., Nagai, R., Yahagi, N., Yamada, I., 2012. Relation between blood pressure estimated by pulse wave velocity and directly measured arterial pressure. *Journal of Robotics and Mechatronics*, 24(5), pp.811-819.
- IEEE Standards Association, 2014. IEEE standard for wearable, cuffless blood pressure measuring devices.
- Kachuee, M., Kiani, M. M., Mohammadzade H., Shabany M., 2015. Cuff-less high-accuracy calibration-free blood pressure estimation using pulse transit time. *2015 IEEE International Symposium on Circuits and Systems (ISCAS)*.
- Legarreta, I.R., Addison, P. S., Reed, M. J., Grubb, N., Clegg, G. R., Robertson, C. E., Watson, J. N., 2005. Continuous wavelet Transform modulus maxima analysis of the electrocardiogram: beat characterisation and beat-to-beat measurement. *International Journal of Wavelets, Multiresolution and Information Processing*, 03(01), pp.19–42.
- Lopez, G., Shuzo, M., Ushida, H., Hidaka, K., Yanagimoto, S., Imai, Y., Kosaka, A., Delaunay, J. J., Yamada, I., 2010. Continuous blood pressure monitoring in daily life. *Journal of Advanced Mechanical Design, Systems, and Manufacturing*, 4(1), pp.179–186.
- Mourad, J.J., 2008. The evolution of systolic blood pressure as a strong predictor of cardiovascular risk and the effectiveness of fixed-dose ARB/CGB combinations in lowering levels of this preferential target. *Vasc Health Risk Manag*, 4(6), pp.1315–1325.
- Mukkamala, R., Hahn, J., Inan, O. T., Mestha, L. K., Kim, C., Toreyin, H., Kyal, S., 2015. Toward ubiquitous blood pressure monitoring via pulse transit time: theory and practice. *IEEE Transactions on Biomedical Engineering*, 62(8), pp.1879–1901.
- Takazawa, K., Tanaka, N., Fujita, M., Matsuoka, O., Saiki, T., Aikawa, M., Tamura, S., Ibukiyama, C., 1998. Assessment of vasoactive agents and vascular aging by the second derivative of photoplethysmogram waveform. *Hypertension*, 32(2), pp.365–370.
- Wang, L., Pickwell, M. E., Liang, Y. P., Zhang, Y. T., 2009. Noninvasive cardiac output estimation using a novel photoplethysmogram index. *2009 Annual International Conference of the IEEE Engineering in Medicine and Biology Society*, pp.1746-1749.
- World Health Organization, 2014. Global Health Statistics 2014.